

## A PROCESS TO PRODUCE A CONTINUOUS LIQUID METAL STREAM FOR GAS ATOMISATION

*K.A. Pericleous\**, *V. Bojarevics*, *C. Tonry*

*University of Greenwich, London, UK*

*\* e-Mail: k.pericleous@gre.ac.uk*

The heating and melting of reactive alloys in a cold crucible are considered in this study to produce a continuous melt stream as feed to a gas atomiser. A pre-heated rod of material enters the crucible at a rate equal to the amount of mass leaving as a liquid stream through the outlet. An induction coil is used to melt the contents of the crucible, which then pours out as a stream to enter a gas atomizer. The outlet nozzle may be controlled using an induction valve, operating at a different AC frequency. The concept is tested through simulations using titanium and a nickel superalloy as model materials.

### Introduction.

The need for metal powder is increasing exponentially in industry for component manufacturing, especially in the aerospace and transport fields and in processes such as additive manufacturing (AM), sintering, injection moulding, metal powder coating and in hot-isostatic pressing. Typical materials used in aerospace feature metals that are highly reactive in the molten state, such as Ti and its alloys. For this reason, melt contact with ceramic refractory materials either in the crucible walls or the pouring nozzle leads to contamination and must be avoided. With these restrictions in mind, to produce the required feed stream of liquid metal to the atomiser, two methods appear in the literature, both relying on induction melting techniques. The classical Cold Crucible (or Induction-Skull Melting (ISM)) [1, 2] method is one that can be used in batch to melt and pour the metal, with the crucible comprising a series of electrically isolated water-cooled copper fingers. The induction coil surrounding the copper crucible induces current in the crucible fingers and a counter current in the metal charge. That then leads to a repulsive force that minimises the contact between the wall and the liquid metal. Where there is contact, a protective ‘skull’ is formed by solidification. Following a US patent by Kusamichi *et al.* [3], this method has been used recently by Kobelco Ltd. [4] in melting and bottom-pouring titanium as a preliminary step to continuous melt stream production. Stenzel *et al.* [5] further proposed using this technique for reactive ( $\gamma$ -TiAl) metal powder production by combining the cold-crucible idea with plasma torch melting and close-coupled atomisation in the PIGA (Plasma-Melting-Induction-Guiding-Gas Atomization) process. With  $\gamma$ -TiAl as the target, this way alloy elements could be combined and homogenised in a melt pool ahead of atomisation. PIGA claims a production rate of up to 250 kg/h. An alternative contactless method EIGA (Electrode Induction Melting Gas Atomization) [6] totally avoids the crucible, instead melting a pre-alloyed ingot (the electrode) using a conical induction coil. The coil is fed continuously by the electrode as it melts providing an atomising stream to a gas nozzle. EIGA has proved to be particularly suitable for AM powder production, with a mean particle diameter around 50  $\mu\text{m}$  [7] but a rather limited production rate of 50 kg/h. In the present contribution, we combine elements of the EIGA and PIGA techniques by introducing a moving electrode into the melt contained in an ISM crucible, with the added control of an outflow inductive nozzle.

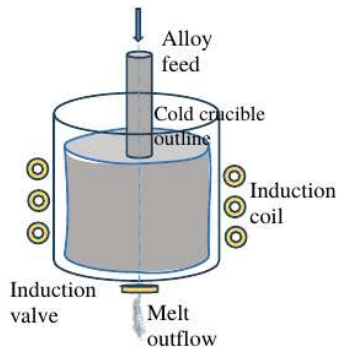


Fig. 1. Continuous melting stream by induction in a cold crucible.

The process conceptually shown in Fig. 1 is simulated using the axisymmetric spectral collocation code SPHINX [8] that combines the elements of physics characterising the process. To optimise operation, the induction coil positioning, current supply and frequency are designed so as to minimise the melt contact with the water-cooled crucible walls, while at the same time generating strong stirring to maintain an even bulk temperature and homogeneity in the melt. For outflow control, a second induction coil operated independently at a suitable frequency is used as a flow control valve. To account for non-axisymmetric effects, e.g., due to coil helicity, the COMSOL code has also been used for detailed magnetic field simulations.

### 1. Setup description.

Considering the EIGA process first, a pre-alloyed rotating feedstock (the solid electrode) is gradually fed into a water-cooled conical induction coil. Induction currents generated by the coil melt a thin film of metal on the periphery of the electrode, which drips down as a thin stream to a gas atomiser. Since only a small amount of metal melts at any time, the current requirement is low. The thin melt stream fed to the atomiser produces fine powder at around  $50\ \mu\text{m}$ , ideal for additive manufacturing. The process is continuous and contactless, which means no contamination from crucible materials. On the negative side, the production rate is quite low, at  $\sim 50\ \text{kg/h}$  resulting in long run times and so expensive powder. Another problem is due to segregations in the length of the feeding electrode resulting in chemically heterogeneous alloy powder.

The simulations in Fig. 2 show the magnetic field lines around the coil and electrode, computed using the COMSOL software, together with the magnetically confined melting process computed using the SPHINX code.

The PIGA process as shown in Fig. 3a (reproduced from Gerling *et al.* [7]) relies on a He-plasma torch to melt the metal in a cold crucible. Alloying takes place in the melt pool and the outflow is through a copper funnel to the atomiser, controlled using an induction coil. With this setup it is possible to achieve a higher production rate, quoted as  $250\ \text{kg/h}$ .

In the present paper, our aim is to combine the best characteristics of the two processes described, ensuring a continuous process for the production of metal powder at a rate faster than EIGA, with better control of the powder alloy composition and removal of oxides and other impurities prior to atomisation. To eliminate the alloying problem and increase the flow rate, a concept as shown in Fig. 3b combining EIGA with a cold crucible is a possibility, albeit a complex one. A simpler arrangement, and the one presented here, is shown in Fig. 3c, where a cold crucible with an EM controlled outlet is

*A process to produce a continuous liquid metal stream for gas atomisation*

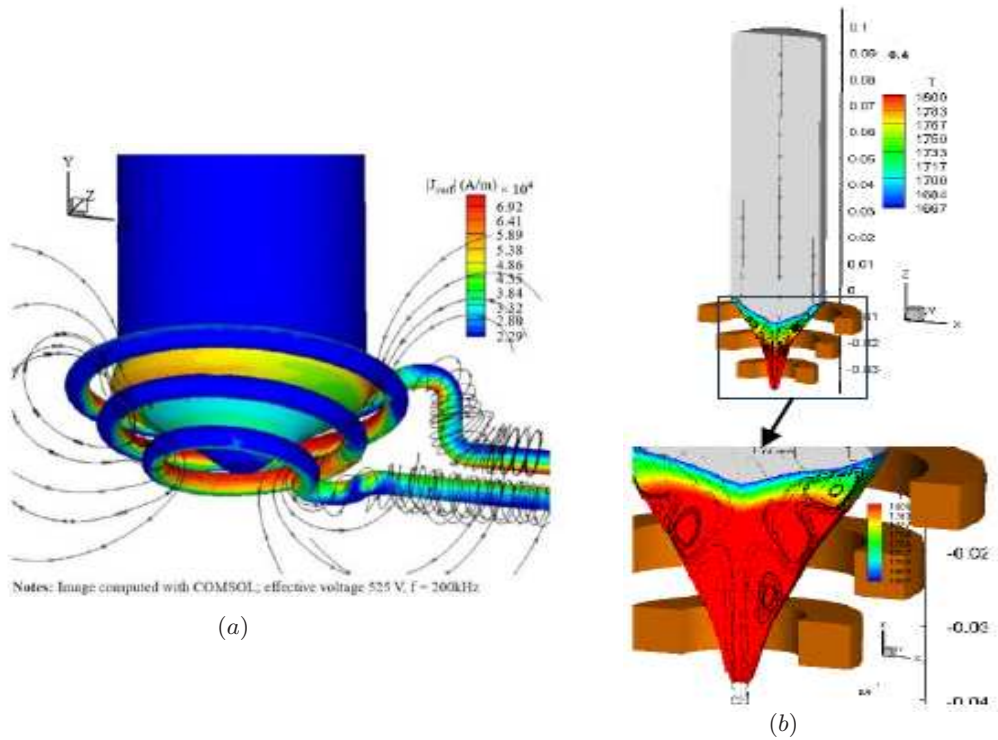


*Fig. 2.* EIGA (a) the magnetic field, (b) the semi-levitating melting process.

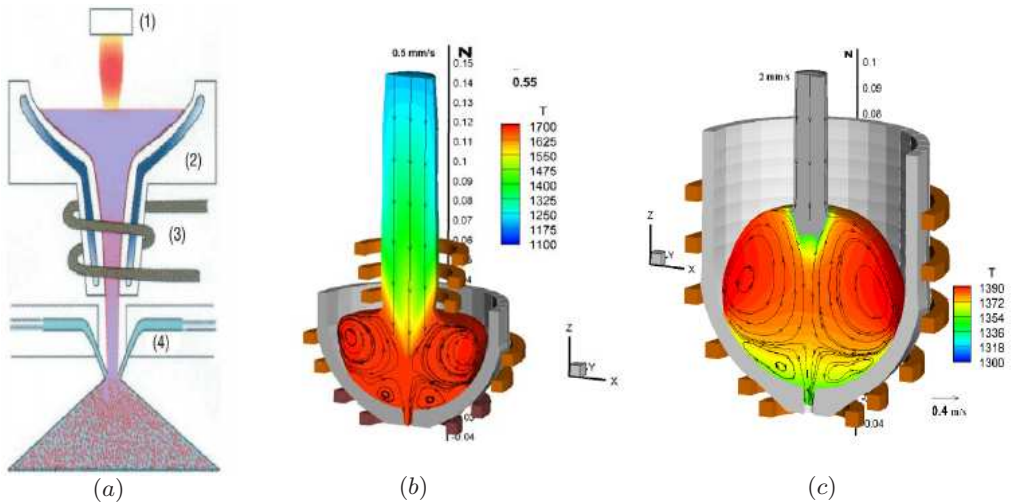


*Fig. 3.* (a) Schematic of the PIGA process [7]: 1 – torch, 2 – crucible, 3 – coil, 4 – atomiser. (b) Extended EIGA. (c) Targeted process for a continuous feed cold crucible.

fed continuously with the base metal rod. Alloying then takes place in the crucible under controlled atmosphere with induction stirring ensuring an even component distribution. The bottom two coil turns in Fig. 3c are operated independently of the main induction coil to allow control of the outflow stream.

## 2. Numerical model.

The momentum and mass conservation equations are solved numerically for incompressible fluid with appropriate effective viscosity  $\nu_e$  and turbulent diffusivity  $\alpha_e$  together with the heat transfer equation:

$$\partial_t \mathbf{v} + (\mathbf{v} \cdot \nabla) \mathbf{v} = -\rho^{-1} \nabla p + \frac{\nabla \cdot (\nu_e (\nabla \mathbf{v} + \nabla \mathbf{v}^T))}{\nabla \cdot \mathbf{v} = 0} + \rho^{-1} \mathbf{f}_{AC} + \mathbf{g}, \quad (1)$$

$$C_p^* (\partial_t T + \mathbf{v} \cdot \nabla T) = \nabla \cdot (C_p \alpha_e \nabla T) + \rho^{-1} |\mathbf{J}|^2 / \sigma. \quad (2)$$

The usual notation is used, given in detail elsewhere [1, 8]. The free surface boundary conditions for velocity vary dynamically with the surface shape and include a no-slip condition at the solid container walls.

$$\mathbf{v} = 0. \quad (3)$$

Referring to Fig. 3c, at the top free surface the normal stress is determined by the pressure  $p_a$  and surface tension  $\Gamma$ ; at the outlet the pressure is prescribed as  $p_b$ :

$$\mathbf{e}_n \cdot \mathbf{\Pi} \cdot \mathbf{e}_n = p_{a,b} + \Gamma K. \quad (4)$$

The outlet pressure  $p_b$  at the nozzle exit could be different from the input  $p_a$ . Additionally, on the liquid metal free surface, the continuity of the velocity field and the tangential stress conditions are prescribed:

$$\nabla \cdot \mathbf{v} = 0, \quad \mathbf{e}_n \cdot \mathbf{\Pi} \cdot \mathbf{e}_\tau = 0, \quad (5)$$

where  $\mathbf{e}_n$ ,  $\mathbf{e}_\tau$  are the unit vectors normal and tangential to the free surface,  $\mathbf{\Pi}$  is the stress tensor,  $K$  the surface curvature. The values of the constant pressure  $p_a$  and  $p_b$  are given for the general statement (in addition to the general boundary conditions (5) and (6)). Normally for the cold crucible melting both of  $p_a$  and  $p_b$  are equal to the same pressure in the vacuum chamber due to the construction of the segmented crucible using gaps between the fingers. However, there are special designs, where the top and bottom chambers are fully isolated and a pressure difference is imposed, then the outflow rate can be additionally controlled. In the present paper, we show only the simplest case, where these  $p_a = p_b = p_a = p_0 = \text{const}$ .

The free surface shape  $\mathbf{R}(t)$  and the liquid contact position to the solid wall are updated at each time step using the kinematic condition:

$$\partial_t \mathbf{R} \cdot \mathbf{e}_n = \mathbf{v} \cdot \mathbf{e}_n. \quad (6)$$

The previously validated [8] ‘ $\kappa$ - $\omega$ ’ turbulence model expanded to include the effects of magnetic damping is used to calculate the effective viscosity  $\nu_e$  and the turbulent thermal diffusivity  $\alpha_e$ . The thermal boundary conditions account for radiation losses and the heat loss to the water-cooled solid surface of the crucible and the nozzle [1, 4, 8].

The axisymmetric spectral code SPHINX computes the electromagnetic force from an integral equation representation. This has an advantage that the boundary conditions are not explicitly required, and the electromagnetic field can be solved only in the regions where it is needed. The electric current  $\mathbf{j}$  distribution in a moving medium of conductivity  $\sigma$  is then given by the magnetic vector potential  $\mathbf{A}$ , the magnetic field  $\mathbf{B} = \nabla \times \mathbf{A}$ , the electric potential  $\varphi$  and the fluid flow induced part  $\sigma \mathbf{v} \times \mathbf{B}$ :

$$\mathbf{j} = \sigma (-\partial_t \mathbf{A} - \nabla \varphi + \mathbf{v} \times \mathbf{B}) = \mathbf{j}_{AC} + \mathbf{j}_v. \quad (7)$$

### A process to produce a continuous liquid metal stream for gas atomisation

The  $\mathbf{j}_{AC}$  part of the current is induced in the conducting medium even in the absence of velocity. The governing integral equations can be obtained [1] from the electric current distribution in the source coils and the unknown induced currents in the liquid are related to the total magnetic field and the vector potential  $\mathbf{A}$  by the Biot–Savart law:

$$\mathbf{A}(\mathbf{r}) = \frac{1}{4\pi} \int \frac{\mathbf{j}(\mathbf{r}')}{|\mathbf{r} - \mathbf{r}'|} d\mathbf{r}'. \quad (9)$$

Eqs. (8) and (9) can be solved efficiently in the axisymmetric case for harmonic fields. The induced current in the liquid depends on its instantaneous free surface shape and needs to be recomputed as the shape changes during melting and pouring. The resulting electromagnetic force  $\mathbf{f}$ , time-averaged over the AC period, similarly to Eq. (8) can be decomposed in two parts:  $\mathbf{f} = \mathbf{f}_{AC} + \mathbf{f}_v$ . The second, velocity-dependent part of the force  $\mathbf{f}_v$  can include both DC and AC time-averaged contributions. In the presence of AC fields originating from different sources such as the main coil at the side of the crucible and the bottom coil at the nozzle, the superposition of the time average force contributions and the Joule heating  $|\mathbf{J}|^2/\sigma$  in the liquid metal are used.

Eqs. (1)–(9) are solved by the spectral collocation method with a Chebyshev grid distribution in the radial direction and Legendre nodes in the vertical direction. The numerical solution method is based on the continuous co-ordinate transformation adapting to the free surface and the containing vessel shape explicitly at consecutive time steps [1]. A stable time integration of the solution requires adjustable time steps of the order 0.1–1 ms for the unsteady fluid flow solution in the examples considered below. A 3D version of the model using COMSOL was also used to check the effects of coil helicity and discrete fingers on the induced magnetic field, as shown in Fig. 4.

### 3. Simulation examples.

Several simulations have been carried out in order to examine the manufacturing potential of this technique, with the scope of supplying a constant stream of liquid metal to the gas atomisation vessel, set here at the rate of 1.5 kg/min.

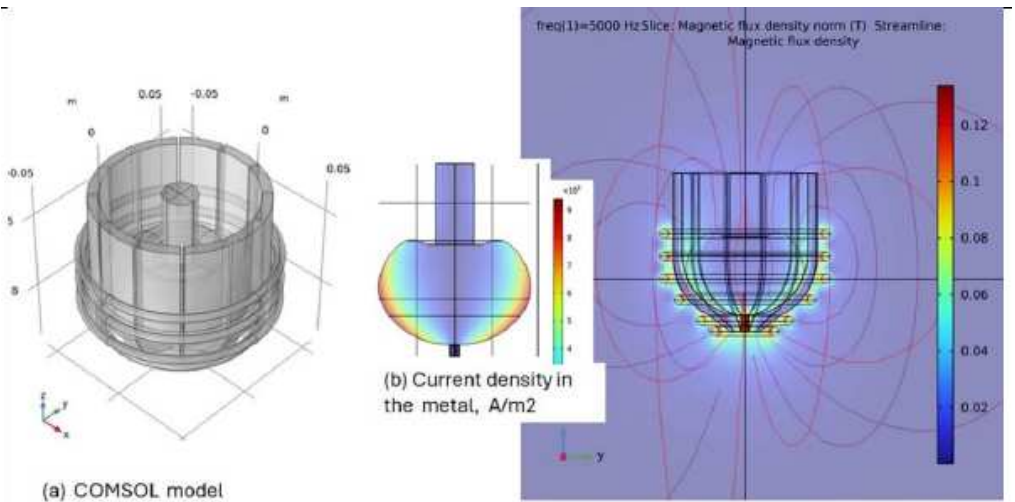


Fig. 4. 3D COMSOL model showing the computed magnetic flux density and the induced current in the melt.

Table 1. Material properties used in the model.

Material properties	Units	Titanium	LEK94
Electrical conductivity	$\Omega^{-1}\text{m}^{-1}$	580000	725000
Density	$\text{kg}/\text{m}^3$	4110	7570
Specific heat	$\text{J}/(\text{kg}\cdot\text{K})$	770	749
Thermal diffusivity, solid	$\text{m}^2/\text{s}$	0.000008	0.00004
Liquidus temperature	$^{\circ}\text{C}$	1670	1393
Solidus temperature	$^{\circ}\text{C}$	1667	1347
Surface tension	$\text{N}/\text{m}$	1.65	1.68
Latent heat	$\text{J}/\text{kg}$	411500	271000
Emissivity	–	0.30	0.27

The shape of the cold crucible is perhaps the most important factor in the overall design, required to melt the charge, minimise the wall contact with the melt, encourage MHD mixing for a uniform temperature and composition and, finally, to facilitate a smooth exit of the atomising stream. For better control of the outlet stream, the two induction coils used can be operated independently. The top coil has four turns, the bottom coil has two turns, fed by independent power sources.

For the examples presented here, a crucible with a hemispherical base was chosen. Metal is fed via a 3-cm diameter cylindrical rod, preheated prior to immersion. Two different aerospace metals were considered, pure titanium and the nickel superalloy LEK94. The material properties of the two alloys are given in Table 1.

The simulation starts ( $t = 0\text{ s}$ ) with the metal filling the crucible at the liquidus temperature and the feed ingot entering at a prescribed rate and temperature. Subsequently, as the Lorentz force and Joule heating enter the process, following initial oscillations, the melt reaches a pseudo-steady domed free surface shape. The solution mesh adapts to the instantaneous melt shape. Heat transfer to the water-cooled walls during contact and the radiative loss from the free surface balance Joule heating and together with flow mixing determine the temperature of the melt. Where the temperature drops below liquidus

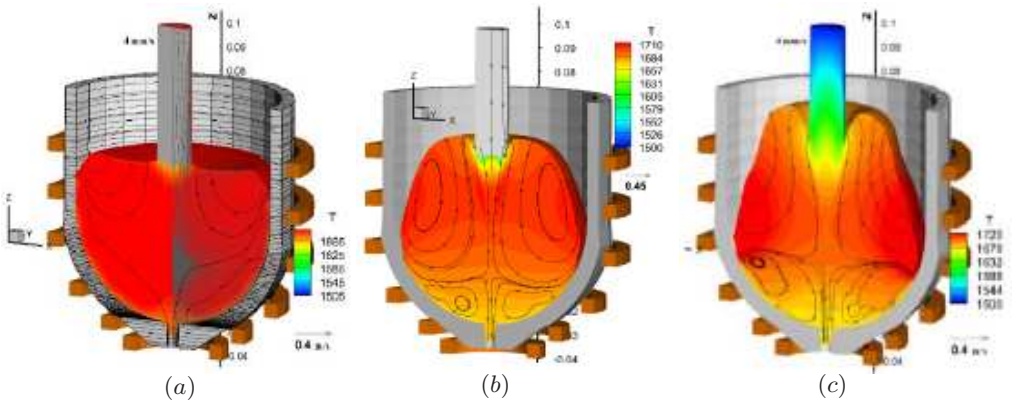


Fig. 5. Ti melting sequence: (a)  $t = 0\text{ s}$ , showing the solution grid and initial melt temperature, (b)  $t = 2\text{ s}$ , the Lorentz force pushes the melt into an oval shape and induces stirring; a preheated electrode is inserted at a rate of  $0.5\text{ mm}/\text{s}$ , as the tip melts it decreases the surrounding temperature and alters the volume envelope (c).

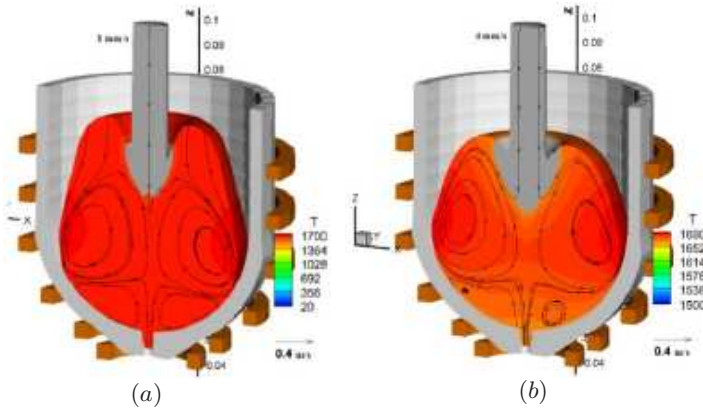
*A process to produce a continuous liquid metal stream for gas atomisation*

either at the outlet or at the ingot injection point, the metal is allowed to solidify. Flow from the outlet occurs when the metal reaches liquidus. Where the melt solidifies on the copper wall surface, a ‘skull’ is formed acting as an additional heat loss path. The effort remains to minimise this solid contact region for maximum efficiency.

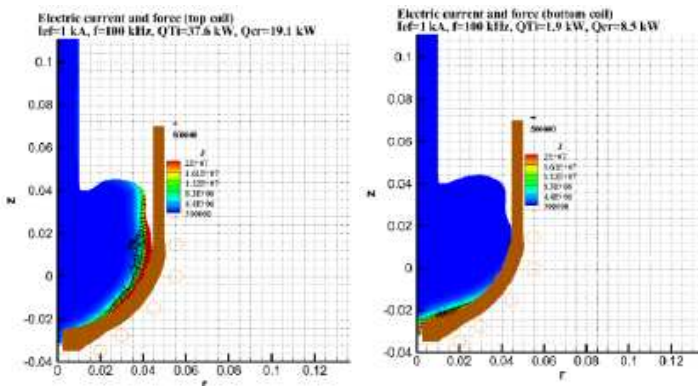
**3.1. Case 1: Ti melt.**

Fig. 5 shows the setup in a cold crucible holding 1.3 kg of Ti at 1700°C. The simulation mesh is created in deformed spherical coordinates (Fig. 5a), and it includes the melt and the electrode. The electrode is preheated to 1000°C prior to insertion; nevertheless, depending on the insertion rate it may re-solidify forming a plug surrounding the tip (Fig. 6).

Fig. 8 demonstrates that a flow stream of 0.15 kg/s can be achieved after ~9s from the feeding rod insertion with the temperature maintained at just above liquidus, 1670°C.



*Fig. 6.* The electrode is preheated to 1000°C, nevertheless, as it enters the melt it, induces local solidification around the tip. Increasing the insertion rate from 1 mm/s to 4 mm/s increases the solid plug and decreases the overall melt temperature.



*Fig. 7.* The instantaneous induced current density, force distribution and the released power in the system at  $t = 15$  s, with both top and bottom coils carrying the same current  $I = 1$  kA at 100 kHz. The top coil (a) supplies 37.6 kW to the melt, while 19.1 kW is lost in the copper crucible (and cooling water). The bottom coil (b), in contrast, supplies just 1.9 kW to the melt, with 8.5 kW going to the crucible.

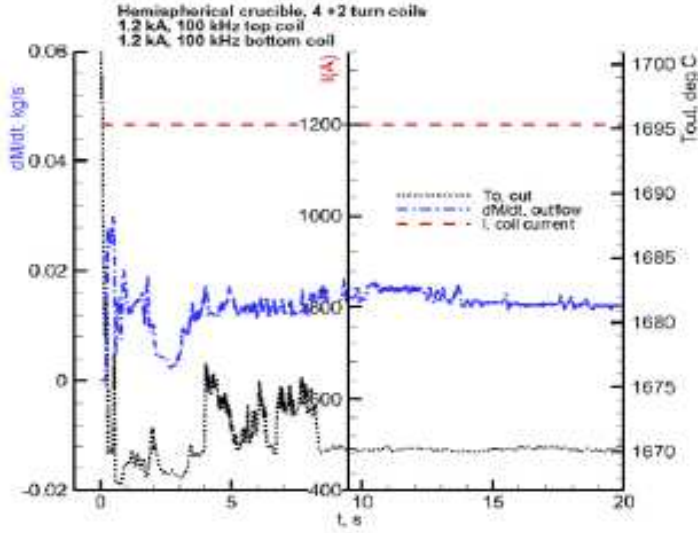


Fig. 8. The computed outflow rate  $dM/dt$  and temperature  $T_0 \sim 1670^\circ\text{C}$  for the coil current  $I = 1.2\text{ kA}$  in both coils. Outflow stabilises after 15 s.

In the Sphinx model, the outflow rate is directly computed by integrating the outflow velocity over the exit nozzle at each time step of the solution, therefore, it is non-stationary, depending on the freezing of the solid film on the cooled Cu wall, the hydrostatic pressure due to the top free surface and the full metal volume change, and the flow turbulence level generated by the time dependent EM force distribution. It is a fully dynamic solution, updated at all time steps continuously.

### 3.2. Case 2: Ni superalloy LEK94 melt.

A similar process is adopted for the LEK94 superalloy, using the material properties given in Table 1. A sample result is illustrated in Fig. 9 at  $t = 10\text{ s}$  following electrode insertion, and the resulting outflow conditions are presented in Fig. 10. Again, a quasi-steady outflow stream of about  $0.03\text{ kg/s}$  is achieved for gas atomisation.

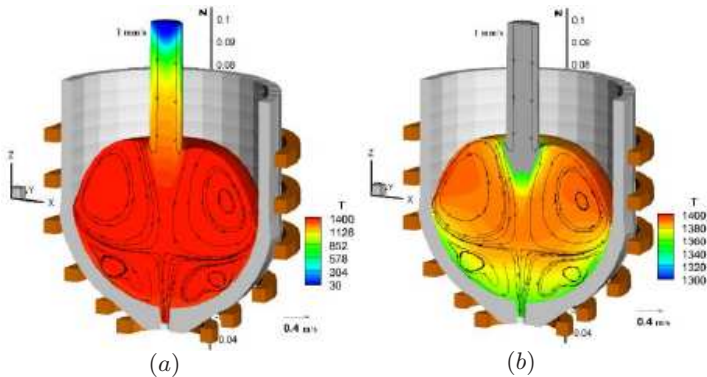


Fig. 9. Nickel alloy melt ( $2.25\text{ kg}$ ) shown after  $10\text{ s}$ . The temperature scale is chosen to show (a) the full temperature range including the 3-cm diameter electrode, and (b) the restricted range for the melt alone, indicating the solid part.

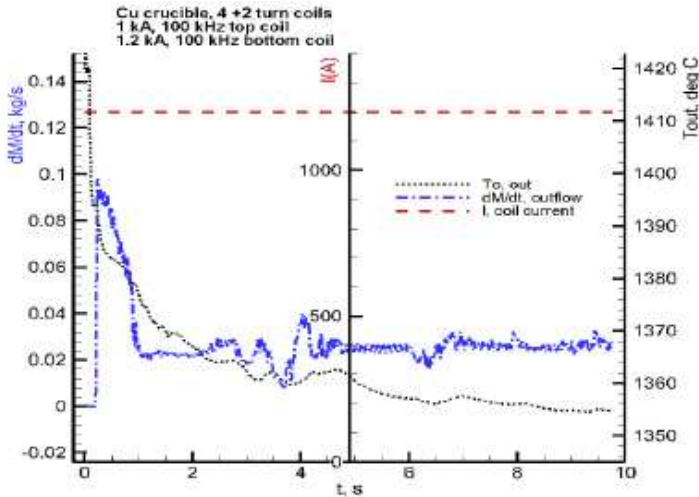


Fig. 10. The computed outflow rate stabilizes at about 0.03 kg/s,  $T_{\text{outflow}} \sim 1355^{\circ}\text{C}$ , the bottom coil current 1.2 kA.

### Conclusions.

This work demonstrates through modelling the possibility of producing a steady stream of liquid metal for gas atomisation by combining induction melting in a cold crucible with a continuously advancing feed rod. With this combination, it is possible to provide and homogenise the correct alloy element proportions in the holding crucible, coupled with a continuous supply of the main metal constituent. In this case, Ti and the LEK94 superalloy were used as examples. To improve control of the outflow and produce a steady melt stream, in addition to the main heating coil, it was found advantageous to employ a second coil to control the outflow nozzle.

### References

- [1] V. BOJAREVICS, K. PERICLEOUS. The Development and experimental validation of a numerical model of an induction skull melting furnace. *Metall. Trans. B*, vol. 35 (2004), pp. 785–803.
- [2] V. BOJAREVICS AND K. PERICLEOUS. Cold crucible melting with bottom pouring nozzle. *COMPEL: The International Journal for Computation and Mathematics in Electrical and Electronic Engineering*, vol. 39 (2019)(1), no. 1, pp. 36–42: DOI: 10.1108/COMPEL-05-2019-0208).
- [3] T. KUSAMICHI *et al.* U.S. Patent # 6, 144,690, 2000.
- [4] V. BOJAREVICS, T. NISHIMURA, D. MATSUWAKA. Development of advanced cold crucible melting of titanium alloys. *Magnetohydrodynamics*, vol. 58 (2022), no. 1, pp. 13–24.
- [5] O.W. STENZEL, G. SICK, M. HOHMANN. German Patent DE 4011 392A1, 1990.
- [6] M. HOHMANN, N. LUDWIG. German Patent DE 4102 101, A1 1991.
- [7] R. GERLING, H. CLEMENS, F. SCHIMANSKY. Power metallurgical processing of intermetallic gamma titanium aluminides. *Advanced Engineering Materials*, vol. 6 (2004), no. 1–2.

- [8] K. PERICLEOUS, V. BOJAREVICS. Pseudo-spectral solutions for fluid flow and heat transfer in electro-metallurgical applications. *Progress in Computational Fluid Dynamics*, vol. 7 (2007), nos. 2/3/4, pp.118–127.

Received 24.11.2024